JOURNAL OF MATERIALS SCIENCE 9 (1974) 744–752

Moisture transport in microporous substances

Part 1 *The interaction of molecular streaming, surface diffusion and capillary suction*

F. RADJY
Building Materials Laboratory, Technical University of Denmark, 2800 Lyngby, Denmark

Steady flow of moisture through a cylindrical pore is analysed in terms of the mechanisms (a) molecular streaming, (b) surface diffusion and (c) capillary suction. The manner in which these mechanisms interact depends on both the surface diffusion coefficient and the pore size. The general character of the derived expressions is investigated for a range of pore sizes and surface diffusion coefficients. Capillary condensation can generally be expected to cause flow amplification of some few orders of magnitude.

1. Introduction

Although many aspects of the transport of sorbable gases and vapours in porous substances have been analysed and are understood in principle [1-3], the role of capillary condensation* has been relatively neglected. The associated transport mechanism, capillary suction, is generally recognized [1, 4, 5] as a flow contributor leading to flow amplification [1] and, in some instances [4, 5], the permeability data have been interpreted solely in terms of this mechanism. However, a detailed investigation of the interaction between capillary suction and various other transport mechanisms has been lacking.

The objective in the following is to consider in detail the transport of moisture through a circular cylindrical pore in a steady state isothermal situation. It is assumed that the transport of moisture occurs by a combination of any of the following mechanisms: (a) surface diffusion; (b) Knudsen flow; (c) capillary suction. Contributions due to Poiseuille flow in the vapour phase are neglected, implying that the pore diameter is sufficiently small compared with the mean free path of water molecules ($\sim$ 4 μm at 25 Torr and 25°C).

The analysis is performed for steady transport through the pore with an imposed relative vapour pressure of zero at the downstream end The upstream relative vapour pressure is varied from zero to unity, and both the fractional length of the pore containing capillary condensate and the flow amplication due to capillary condensation are computed. The computations take into account partial pore blocking due to the adsorbed layer – the "t-layer" – and are performed for different assumed values of the surface diffusion coefficient.

With the development of the t-method of pore structure analysis [6-8], and the recent availability [9] of the "t-isotherm" for water, it is now possible to formulate the problem of moisture transport in microporous substances in terms of the appropriate mechanisms and the pore structure. The flow problem analysed herein is one of the prerequisites to such an undertaking.

2. Basic flow equations and the surface factor

Consider a pore of radius, R, and length, L, as shown in Fig. 1. Start with both the downstream and the upstream sides at a vapour pressure of zero. As the upstream pressure is gradually increased, during an initial period prior to KCC the situation in Fig. 1 will develop; the pore will conduct moisture by surface diffusion

*Hereafter denoted by KCC = (Kelvin) Capillary Condensation.

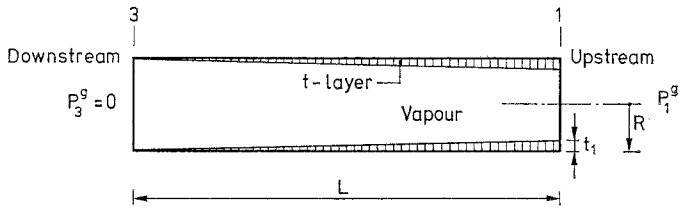

Figure 1 Cylindrical pore with adsorbed t-layer prior to capillary condensation. The t-profile need not be linear.

through the t-layer and by Knudsen flow through the vapour phase.

According to the t-method [8] of pore structure analysis, the condition for KCC is that

$$R = t(h) + r(h)\,, \tag{1}$$

where t is the adsorbate layer thickness at the given relative vapour pressure $h(= P^g/P_s{}^g)$ as obtained from the appropriate t-isotherm, $r(h)$ is the corresponding Kelvin radius, and the contact angle is taken as zero. The parameters r and h are related by the Kelvin equation [10]

$$\frac{1}{r} = -\frac{\mathscr{R}T}{2\sigma v^l}\ln h\,, \tag{2}$$

where $\mathscr{R}$ is the gas constant, T the absolute temperature, σ the vapour/liquid interfacial tension, and v^l the molar volume of the capillary liquid. The solution of Equation 1 in the form $h(R)$ for a given pore size R then gives the critical vapour pressure h_R beyond which KCC is expected to occur, presuming that there are no hysteresis effects.

The situation which develops after the upstream relative vapour pressure, h_1, has exceeded h_R is depicted in Fig. 2. Moisture conduction is now by a compound series/parallel process. In the section "12" moisture is transported by capillary suction. This conduction occurs in series with the parallel transport occurring in the t-layer and the vapour phase in the "23" section.

When the pore of Figs. 1 or 2 is considered as a black box, moisture conducting device, the appropriate transport equation is [3]

$$\bar{P}_{13}{}^g \cdot q_{13} = \bar{K}_{13}\frac{\Delta P_{13}{}^g}{L}\,, \tag{3}$$

where $\bar{P}_{13}{}^g$ is the mean vapour (gas) pressure across the "13"-section, q_{13} the linear flow velocity (cm sec^{-1}) or the volume flux (cm^3 cm^{-2} sec^{-1}), referred to the mean pressure $\bar{P}_{13}{}^g$, $\bar{P}_{13}{}^g q_{13}$ the overall flux in pressure-volume (PV)

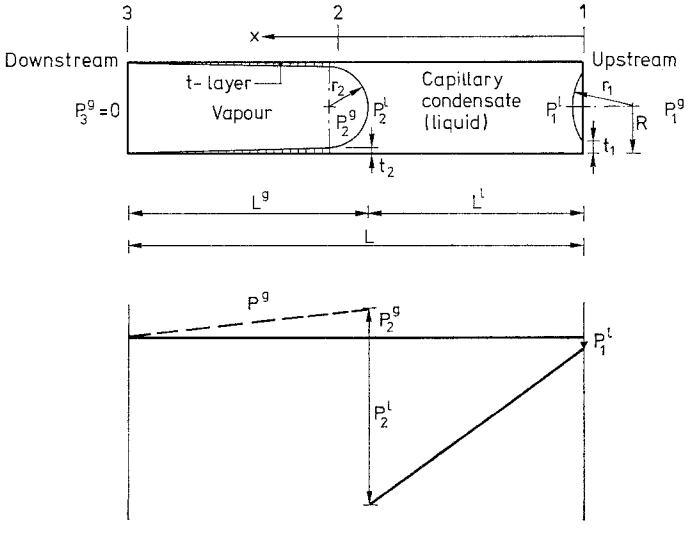

Figure 2 Pore of Fig. 1 after capillary condensation (top), and pressure profiles (bottom). The P^g and t-profiles need not be linear.

units; $\bar{K}_{13}$ the effective (PV−) permeability at the mean pressure $\bar{P}_{13}{}^{g}$ (cm² sec⁻¹) and $\Delta P_{13}{}^{g} = P_1{}^{g} - P_2{}^{g}$. This overall permeability, $\bar{K}_{13}$, must now be related to the internal processes which transport the moisture.

Referring to Fig. 2, first consider the liquid filled section "12". Assuming Poiseuille flow with no slip at the boundary, the transport equation is

$$q_{12}{}^{l} = \frac{R^2}{8\eta^{l}} \cdot \frac{\Delta P_{12}{}^{l}}{L^{l}}, \tag{4}$$

where $q_{12}{}^{l}$ is the volume flux (cm³ cm⁻² sec⁻¹), R the pore radius, η^{l} the viscosity of the capillary condensate and $\Delta P_{12}{}^{l} = P_1{}^{l} - P_2{}^{l}$. Or, writing Equation 4 in terms of the mass flux $J_{12}{}^{l}$ (g cm⁻² sec⁻¹), one obtains

$$J_{12}{}^{l} = \rho^{l} \cdot q_{12}{}^{l} = \frac{\rho^{l} R^2}{8\eta^{l}} \cdot \frac{\Delta P_{12}{}^{l}}{L^{l}}, \tag{5}$$

where ρ^{l} is the mass density of the capillary condensate.

In the "23"-section of Fig. 2, the contribution to flow by molecular streaming in the gas phase is

$$J_{23}{}^{g} = \frac{M \bar{K}_{23}{}^{g}}{\mathscr{R}T} \frac{\Delta P_{23}{}^{g}}{L^{g}}, \tag{6}$$

where $J_{23}{}^{g}$ is the mass flux, M the molecular weight, $\bar{K}_{23}{}^{g}$ the effective Knudsen permeability, and $\Delta P_{23}{}^{g} = P_2{}^{g} - P_3{}^{g}$. For a cylinder of uniform radius, a, the Knudsen (PV−) permeability K^{g} is given [2] by

$$K^{g} = \frac{2}{3} \bar{v} a \cdot \frac{2 - f}{f}, \tag{7}$$

where $\bar{v}$ is the mean thermal velocity of the gas molecules given by

$$\bar{v} = \left[\frac{8\mathscr{R}T}{\pi M}\right]^{1/2}, \tag{8}$$

and f is the proportion of molecules which undergo diffuse reflection at the pore walls. Now it is assumed that (1) $f \simeq 1$ in line with the general practice [2, 3]; and (2) the effective pore radius for Knudsen flow is $(R - \bar{t}_{23})$, where $\bar{t}_{23} = (t_2 - t_3)/2$. Thus one obtains

$$\bar{K}_{23}{}^{g} = \frac{2}{3} \bar{v} (R - \bar{t}_{23}). \tag{9}$$

In the "23"-section there is also a contribution to flow due to surface diffusion, given by (see Appendix 1)

$$J_{23}{}^{\sigma} = \frac{\Delta \Gamma_{23}}{\Delta P_{23}{}^{g}} \langle D^{\sigma} \rangle_{23} \cdot \frac{\Delta P^{g}{}_{23}}{L^{g}}, \tag{10}$$

where Γ is the surface concentration as obtained from the t-isotherm, $\Delta \Gamma_{23} = \Gamma_2 - \Gamma_3$, and $\langle D^{\sigma} \rangle_{23}$ is the surface concentration average of the surface diffusion coefficient in the interval $\Gamma_2 - \Gamma_3$.

The total flux, J_{23}, in the "23"-section is now obtained by combining the total flows (g sec⁻¹) contributed by the fluxes of Equations 6 and 10, and dividing by the flow cross-section πR^2:

$$J_{23} = (1 - \bar{t}_{23}/R)^2 \cdot J_{23}{}^{g} + \frac{2}{R} J^{\sigma}. \tag{11}$$

It is convenient to relate J_{23} to its conjugate gradient, $\Delta P_{23}{}^{g}/L^{g}$, by a transport coefficient involving the uncorrected Knudsen flow permeability $K_0{}^{g}$ – as if there were no pore blocking and no surface diffusion – given by

$$K_0{}^{g} = \frac{2}{3} \bar{v} R, \tag{12}$$

and a function, Ω, which accounts for deviations from simple molecular streaming. Combination of Equation 6 and 9 to 12 leads to

$$J_{23} = \Omega_{23} \frac{M}{\mathscr{R}T} K_0{}^{g} \frac{\Delta P_{23}{}^{g}}{L^{g}}, \tag{13}$$

where Ω_{23} is the aforementioned function

TABLE I Surface factor Ω_{23}

		D^{σ} (cm² sec⁻¹)					
R (Å)	h_R	10^{-8}	10^{-7}	10^{-6}	10^{-5}	10^{-4}	10^{-3}
20	0.50	0.706	1.16	5.71	51.2	506	5050
50	0.782	0.786	0.857	1.57	8.69	79.9	792
100	0.89	0.855	0.875	1.08	3.08	23.2	224
200	0.947	0.911	0.917	0.973	1.54	7.16	63.4
500	0.978	0.958	0.959	0.969	1.07	2.09	12.2
1000	0.990	0.975	0.975	0.978	1.01	1.30	4.25

appropriate to the "23"-section, referred to as the "surface factor", and defined by

$$\Omega_{23} = \left(1 - \frac{\bar{t}_{23}}{R}\right)^3 + \frac{3\mathscr{R}T}{M\bar{v}P_s{}^g} \cdot \frac{\Delta\Gamma_{23}}{\Delta h_{23}} \frac{1}{R^2}\langle D^\sigma\rangle_{23}, \quad (14)$$

where $h = P^g/P_s{}^g$, and $\Delta h_{23} = h_2 - h_3 \equiv h_R$. The first term in Equation 14 is always less than or equal to unity and accounts for flow attenuation due to pore blocking. The second term is always a positive contribution due to surface flow. As will be demonstrated shortly (Table I), the surface factor can in practice range from an order of unity to a few thousand.

3. The filling transition and flow amplification

Since the conductions in the "23"- and the "12"-sections are in series, and steady state conditions are assumed, the flux balances

$$J_{13} = J_{12}{}^l \quad (15)$$

$$J_{13} = J_{23} \quad (16)$$

apply. Equations 13 and 16 result in

$$J_{13} = \Omega_{23}\left(1 + \frac{1}{\beta}\right)\frac{\Delta P_{23}{}^g}{\Delta P_{13}{}^g} \cdot \frac{M}{\mathscr{R}T} \cdot K_0{}^g \cdot \frac{\Delta P_{13}{}^g}{L}, \quad (17)$$

where β is the ratio L^g/L^l. A comparison of Equations 3 and 17, and using the facts that PV-flux = (mass flux) $(\mathscr{R}T/M)$, $h_2 \equiv h_R$ and $h_3 = 0$, leads to

$$\bar{K}_{13} = \Omega_{23}\left(1 + \frac{1}{\beta}\right)\frac{h_R}{\Delta h_{13}} \cdot K_0{}^g, \quad (18)$$

which relates the overall, measurable permeability $\bar{K}_{13}$ to the characteristics of the assumed, internal transport mechanisms. In the absence of KCC, denoting the overall permeability by $\bar{K}^0{}_{13}$, and noting that $1/\beta = L^l/L^g = 0$ and sections "2" and "1" are identical, from Equation 18 one obtains

$$\bar{K}_{13}{}^0 = \Omega_{13}K_0{}^g, \quad (19)$$

which applies to a situation such as Fig. 1, irrespective of whether KCC has not occurred due to too low a vapour pressure ($h_1 < h_R$) or due to hysteresis effects. Equation 14 with subscript "2" replaced by "1" is used to compute Ω_{13}.

An alternative expression for $\bar{K}_{13}$ is obtained by using Equations 2, 3, 5 and 15 together with the Laplace equation [10],

$$\Delta P_{12}{}^l = 2\sigma\left(\frac{1}{r_2} - \frac{1}{r_1}\right). \quad (20)$$

The result is expressed by

$$\bar{K}_{13} = \frac{1}{8\eta^l P_s{}^g}\left(\frac{\mathscr{R}T}{v^l}\right)^2 \cdot \frac{R^2}{\Delta h_{13}} \cdot \ln\left(\frac{h_1}{h_R}\right) \cdot (1 + \beta). \quad (21)$$

The parameter β is a measure of the extent of KCC; it is zero for a full pore and infinity for a pore totally lacking in the capillary condensate. The β-parameter is obtained by equating the two expressions, Equations 18 and 21, for $\bar{K}_{13}$ and using Equation 12:

$$\beta = \frac{16\eta^l\bar{v}P_s{}^g}{3}\left(\frac{v^l}{\mathscr{R}T}\right)^2 \cdot \frac{\Omega_{23}}{R} \cdot \frac{h_R}{\ln(h_1/h_R)}, \quad (22)$$

where the condition $h_3 = 0$, giving $\Delta h_{23} \equiv h_R$, has also been asserted. Equation 22 forms the basis for computing the "fill-ratio", L^l/L, according to the relationship

$$L^l/L = (1 + \beta)^{-1}. \quad (23)$$

Another parameter of interest is the flow amplification factor α, defined by the ratio $\bar{K}_{13}/\bar{K}_{13}{}^0$ and given by

$$\alpha = \frac{\Omega_{23}}{\Omega_{13}}\left(1 + \frac{1}{\beta}\right)\frac{h_R}{\Delta h_{13}}. \quad (24)$$

4. Numerical estimates

In order to ascertain the general character of some of the parameters derived above, numerical computations were undertaken for a particular water vapour t-isotherm, and a range of pore sizes and surface diffusion coefficients. Only typical features of this numerical analysis, performed by a digital computer, will be included here.

The t-curve chosen has been reported by Hagymassy *et al* [9], applies to adsorbents with a BET C-value in the range 23 to 200, and is probably appropriate for such materials as hardened cement paste and porous glass. Fig. 3 is a plot of this t-curve, together with the Kelvin radius from Equation 2 and the pore radius from Equation 1. The data apply at $T = 298$ K. For a given pore radius, R, the relative vapour pressure h_R is read from the graph (e.g. $h_{20} = 0.5$).

Throughout the calculations a monolayer thickness of 3 Å and a molecular area of 11.4 Å

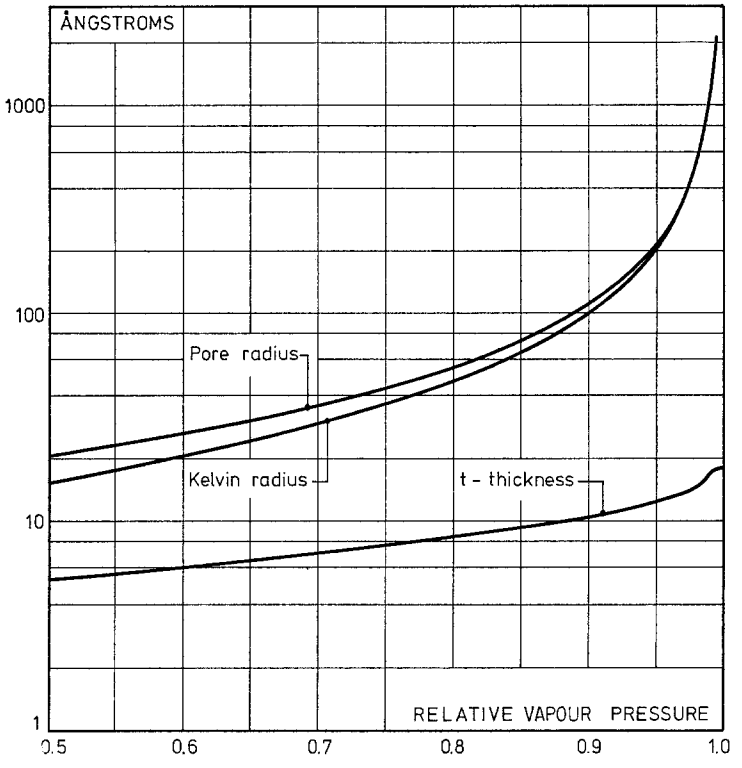

Figure 3 Pore radius, Kelvin radius and the t-thickness for a circular cylindrical pore adsorbing water vapour at 25°C. t-isotherm from [9], $C = 23$ to 200.

were used. The surface concentration Γ(g cm^{-2}) was obtained from

$$\Gamma = \frac{M}{N_{AV} \cdot A_m} \cdot \theta , \qquad (25)$$

where M is the molecular weight, N_{AV} Avogado's number, A_m the molecular area, and θ the adsorbate content in statistical monolayers.

The surface diffusion coefficients assumed were in the range from 10^{-8} to 10^{-3} cm^2 sec^{-1}, at intervals of one order of magnitude. The choice was motivated by the observation that most effective and surface diffusion coefficients reported in the literature [1, 2, 11-14] for various adsorbate-adsorbent systems lie in this range. In particular for systems in which water [11-13] is the adsorbate, the orders of magnitude of the diffusion coefficients lie in the range from 10^{-8} to 10^{-5} cm^2 sec^{-1}.

Table I lists the surface factor Ω_{23} (Equation 14) appropriate to the pore region ahead of the meniscus (Fig. 2) as a function of pore radius and surface diffusion coefficient. In the absence of both pore blocking due to the t-layer and surface diffusion, Ω will equal unity. Pore blocking tends to reduce Ω from its Knudsen value of unity, while surface diffusion will increase Ω. As would be expected, Table I shows that the above effects are much more pronounced in the small pores. It is further seen that the tempting approximation of setting Ω equal to unity is not generally justifiable.

Fig. 4, based on Equations 22 and 23, demonstrates the extent of KCC as a function of the upstream relative vapour pressure (downstream vapour pressure $\equiv 0$) for different combinations of pore size and surface diffusion coefficient. It is seen that for cases where the surface factor is of the order of unity (see Table I), the pore fills with capillary condensate rather rapidly, the filling process approaching a step-like transition. The concurrent flow amplification, based on Equation 24, is demonstrated by Fig. 5. The extent of this amplification is again seen to be sensitive to the surface factor (Table I): when the surface factor is relatively low, KCC amplifies the

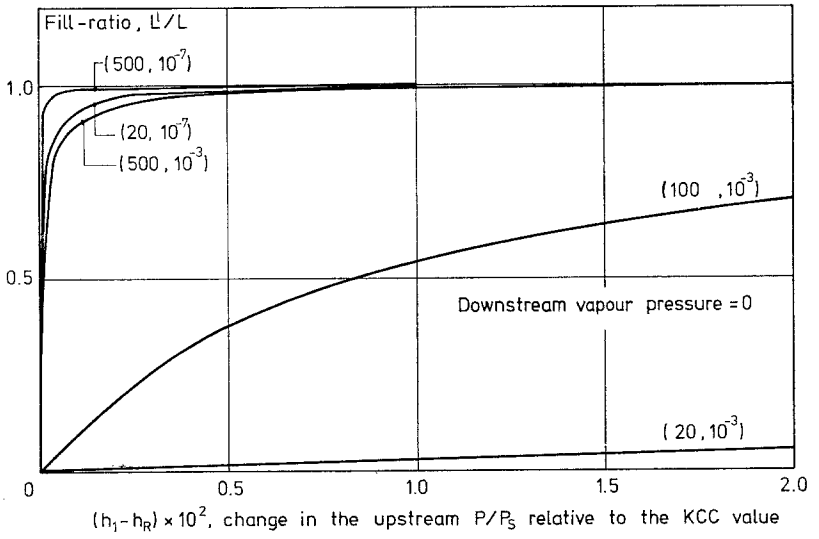

Figure 4 Extent of capillary condensation (fill-ratio) as a function of upstream relative vapour pressure. In parentheses: pore radius in Å, surface diffusion coefficient in $cm^2\ sec^{-1}$.

flow substantially – to over three orders of magnitude.

5. Limiting flow

In the analysis so far it has been assumed that the flux balance $J_{23} = J_{12}{}^{l}$ (Equations 15 and 16), can be satisfied while: (1) the mean free path λ satisfies the requirement $\lambda \ll L^g$ so that Equation 6 will apply; (2) the internal capillary meniscus has not reached the end "1" so that the internal Kelvin radius is given by $r_2 = R - t_2$. For a given situation, then, the only adjustment allowed for achieving flux balance has been the length L^l (or L^g). If the liquid flux $J_{12}{}^{l}$ is too high, L^l would be increased in order to simultaneously decrease $J_{12}{}^{l}$ (lower gradient) and increase J_{23} (smaller L^g, hence larger gradient).

As the fill-ratio L^l/L approaches unity, which can happen for cases with a surface factor of the order of unity, the restriction $\lambda \ll L^g$ may be violated. Furthermore, what if the fill-ratio is exactly unity and still $J_{12}{}^{l} > J_{23}$?

First consider the limiting case of a full pore ($L^l/L = 1.0$), depicted in Fig. 6 and subject to the restrictions that (1) the surface factor is unity, and (2) the upstream end is exposed to a saturated atmosphere ($h_1 = 1.0$). Assumption (1) is justified by noting from Tables I and II that a fill-ratio close to unity can be expected only for cases where the surface factor is of the order of unity. If there is a possibility that the flux balance cannot be satisfied, i.e. $J_{12}{}^{l} > J_{23}$, keeping $h_1 = 1.0$ (assumption 2) maximizes this possibility since the corresponding liquid phase flux will have its maximum value. The liquid phase flux J^{l*} under these conditions is given by

$$J^{l*} = \frac{\rho^l \sigma}{4\eta^l} \cdot \frac{R - t_2}{L}, \qquad (26)$$

TABLE II Fill-ratio with upstream at saturation

		D^σ ($cm^2\ sec^{-1}$)					
R (Å)	h_R	10^{-8}	10^{-7}	10^{-6}	10^{-5}	10^{-4}	10^{-3}
20	0.5	0.9999	0.9998	0.9990	0.9914	0.9212	0.5393
50	0.782	0.9998	0.9997	0.9995	0.9974	0.9767	0.8089
100	0.89	0.9997	0.9997	0.9996	0.9989	0.9918	0.9257
200	0.947	0.9996	0.9996	0.9996	0.9994	0.9971	0.9748
500	0.978	0.9996	0.9996	0.9996	0.9996	0.9991	0.9950
1000	0.990	0.9995	0.9995	0.9995	0.9995	0.9994	0.9980

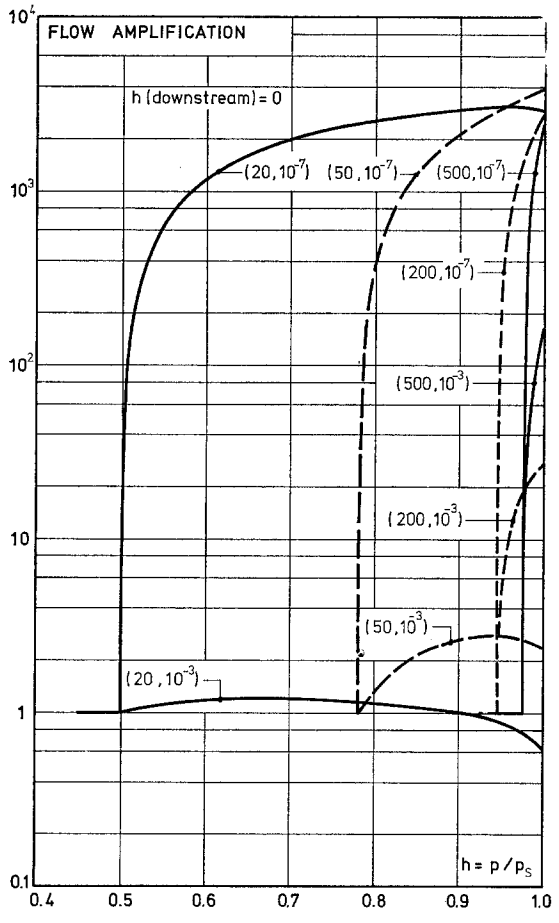

Figure 5 Flow amplification as a function of the upstream relative vapour pressure, In parentheses: see Fig. 4 caption.

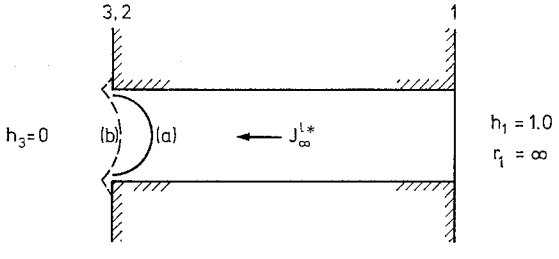

Figure 6 Full tube flow. (a) Tube is just full. (b) Meniscus adjustment.

where Equations 5 and 20 have been used. The corresponding gas phase flux, J^{g*} is obtained by using the kinetic theory expression that the molecular flux in a given direction is $n\bar{v}/4$, where n is the gaseous molecular density and $\bar{v}$ the thermal velocity. Application of this expression to the gas molecules adjacent to the meniscus, results in

$$J^{g*} = \frac{M\bar{v}P_s{}^g}{4\mathscr{R}T} h_R . \tag{27}$$

It can be stated that if $J^{l*} < J^{g*}$, the full tube condition being considered will not arise, since meniscus recession (from the end "3") will eventually produce a flux balance. On the other hand, if $J^{l*} > J^{g*}$, the only degree of freedom remaining would be a curvature adjustment of the meniscus by allowing a position as shown in Fig. 6; the pore edges are used for meniscus curvature control [10]. Fig. 7 is a graphical presentation of Equations 26 and 27, showing that for pores of the order of 1 mm or longer in length and 1000 Å or larger in pore radius, the limiting, full tube liquid flux J^{l*} will be less than the corresponding gas phase flux J^{g*}. Accordingly, except for very thin sections, the general premises of the analyses of the previous sections are justified.

An apparent remaining problem is, however, the applicability of the Knudsen equation (Equation 6) in cases of almost full pores ($L^g \sim \lambda$). The overall permeability $\bar{K}_{13}$ of Equation 21, apart from through β, is independent of the Knudsen assumptions since it is based on the liquid phase flux. The computations of β (Equation 22), the fill-ratio (Equation 23), and the amplification factor, (Equation 24), however, assume the validity of the Knudsen equation. In the case of $L^g \to 0$, the apparent gas phase flux given by Equation 6 will tend to infinity, whereas the true limiting gas phase flux is given according to Equation 27 and is finite. Equation 6 in its region of inapplicability, therefore, overestimates the gas phase flux. Accordingly, in cases where pore filling appears to be occurring rapidly (Fig. 4, surface factor ~ 1.0) when the analysis is based on Equation 6, a more correct analysis will lead to an even sharper filling tansition. Also, if the permeability of Equation 21 is to be obtained when the fill-ratio is almost unity, $\beta \sim 0$, no serious error is incurred by either setting β equal to zero in Equation 21, or using an incorrect value of (say) 10^{-3} instead of a true value of (say) 10^{-4}.

6. Discussion and conclusions

Both the degree of pore filling and flow amplification due to capillary condensation are sensitive to the surface diffusion coefficient. Depending

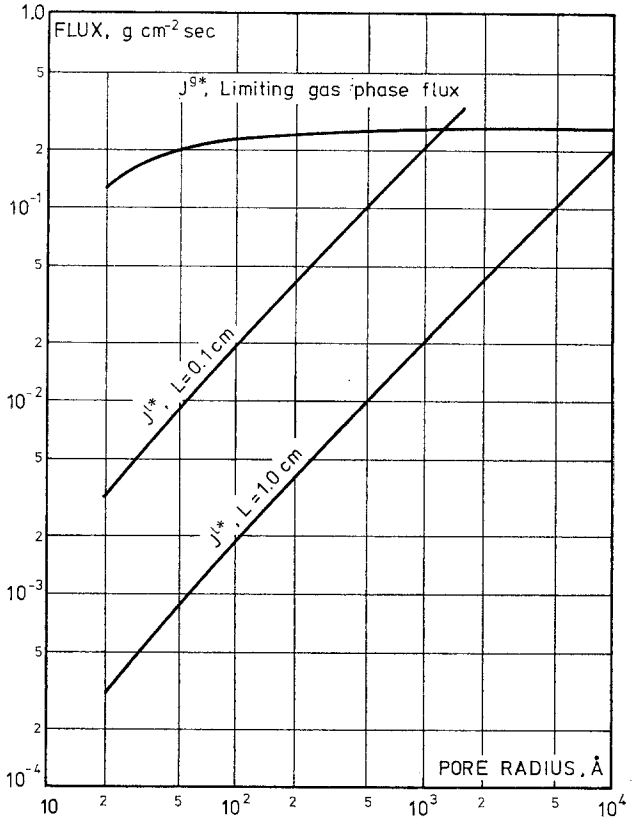

Figure 7 Limiting fluxes.

on the surface diffusion coefficient, D^σ, and the pore size, the flow amplification factor can range from unity ($D^\sigma \simeq 10^{-3}$ cm^2 sec^{-1}) to over three orders of magnitude ($D^\sigma \simeq 10^{-7}$ cm^2 sec^{-1}). In cases of low surface diffusion coefficients, pore filling during steady transport due to capillary condensation can occur as a step-like transition as a function of the upstream vapour pressure.

The analysis has been restricted to the case of molecular streaming in the gas phase, neglecting gas phase transport due [2] to Poiseuille flow and conduction. In a particular application (given pore size distribution) if necessary, however, the analysis can easily be modified to include the more generalized considerations discussed by Barrer [2].

The main intention has been to lay the foundation for a proper interpretation of moisture permeability data in microporous substances. It is evident that this analysis can, in principle, be combined with pore structure data as obtained from the *t*-method [8] to establish a self-consistent framework for relating pore structure to moisture transport by numerical-techniques, a matter which will be the subject of a future publication.

Appendix 1. The surface flux

Referring to Fig. 2, the steady surface flux $J_{23}{}^\sigma$ (g cm^{-1} sec^{-1}) in the "23"-section is given by

$$J_{23}{}^\sigma = - D^\sigma \frac{\partial \Gamma}{\partial x} \cdot \qquad \text{(A1)}$$

where D^σ is the surface diffusion coefficient, Γ the surface concentration (g cm^{-2}) and x is measured along the pore length. Following the method of Carman [1, p. 2], integrate Equation A1 from $x = x_2$ to $x = x_3$ and obtain

$$J_{23}{}^\sigma = \langle D^\sigma \rangle_{23} \cdot \frac{\Gamma_2 - \Gamma_3}{L^g}, \qquad \text{(A2)}$$

where $L^g = x_3 - x_2$ and $\langle D^\sigma \rangle_{23}$ is the concentration average of D^σ given by

$$\langle D^\sigma \rangle_{23} = \frac{1}{\Gamma_2 - \Gamma_3} \int_{\Gamma_2}^{\Gamma_3} D^\sigma \mathrm{d}\Gamma. \qquad \text{(A3)}$$

References

1. P. C. CARMAN, "The Flow of Gases Through Porous Media" (Academic Press, New York, 1956) pp.104-138.
2. R. M. BARRER, "The Solid-Gas Interface", edited by E. A. Flood (Marcel Dekker, New York, 1967) pp. 557-609.
3. D. M. GROVE, "Porous Carbon Solids", edited by R. L. Bond (Academic Press, New York, 1967) pp. 155-202.
4. A. E. SCHEIDEGGER, "The Physics of Flow Through Porous Media" (Oxford University Press, London, 1963) p. 187.
5. H. J. MOREL-SEYROUX, "Flow Through Porous Media", edited by R. J. M. DeWeist (Academic Press, New York, 1969) pp. 456-516.
6. B. C. LIPPENS and J. H. DeBOER, *J. Catalysis* **4** (1965) 319.
7. R.SH. MIKHAIL, S. BRUNAUER and E. E. BODOR, *J. Colloid and Interface Sci.* **26** (1968) 45.
8. F. RADJY and E. J. SELLEVOLD, *ibid* **39** (1972) 367.
9. J. HAGLYMASSY, JUN, S. BRUNAUER and R.SH. MIKHAIL, *ibid* **29** (1969) 485.
10. R. DEFAY, I. PRIGOGINE, A. BELLEMANS and D. H. EVERETT, "Surface Tension and Adsorption" (John Wiley and Sons, New York, 1966) pp. 220, 7, 223 (order of reference in text).
11. C. PARRAVANO, J. D. BALDESCHWIDER and M. BONDART, *Science* **155** (1967) 1535.
12. W. H. BRAY, "Diffusion of Water in Hardened Cement Paste", Technical Report 112, Dept. of Civil Engineering, Stanford University, California (1969) pp. 166-167.
13. W. KAST and F. JOKISCH, *Chemie-Ingenieur-Technik* **44** (1972) 556.
14. B. BODDENBERG, R. HAUL and G. OPPERMANN, *J. Colloid and Interface Sci.* **38** (1972) 210.

Received 26 September and accepted 8 November 1973.